

## Effects of crustal heterogeneity on the morphology of chasmata, Venus

Leslie F. Bleamaster III<sup>1</sup>

Department of Geological Sciences, Southern Methodist University, Dallas, Texas, USA

Vicki L. Hansen

Department of Geological Sciences, University of Minnesota Duluth, Duluth, Minnesota, USA

Received 3 October 2003; revised 17 December 2003; accepted 2 January 2004; published 14 February 2004.

[1] The Ix-Chel, Kuanja, and Vir-ava Chasmata (IKVC) are a 7000-km-long collection of discontinuous topographic troughs and deformation suites. Collectively, they account for approximately 12.5% of the ~55,000 linear km of chasmata on Venus; however, morphologically the IKVC differs significantly from the majority (75%) of Venusian chasmata because it lacks corona features. Coronae represent notable volumes of material both erupted onto the surface and intruded into the crust. Together with chasmata, coronae may also be important indicators of Venus's interior convective processes as well as significant contributors to Venus's heat loss. Although IKVC lacks coronae, detailed geologic and structural mapping along its length highlights previously unrecognized structural and volcanic relationships indicative of local uplift, collapse, and volcanism we call pseudocorona. In light of this mapping, previous corona formation models (theoretical and numerical) are evaluated, and an amended hypothesis (diapir stagnation) is presented for pseudocorona formation. The diapir stagnation model proposes that variations of the crustal thickness perturb corona formation and thus affect their resultant surface morphology. Chasmata are accompanied by corona development when forming in regions of relatively thin, or normal (plains-type), crust (<20 km) but lack corona features when influenced by crustal heterogeneities (mechanical and chemical) at depth associated with thick crustal plateau roots (35–80 km (e.g., Ovda, Thetis, and Phoebe Regios)). Beneath crustal plateaus, diapiric rise is inhibited by (1) the presence of a low-density crustal keel that creates a deep-seated density trap and (2) a composition-dependent mechanically weak crust-mantle boundary layer. Diapir stagnation can be characterized or accompanied by minimal broad doming of the surface, formation of radial and concentric extension structures, lateral dike propagation, and collapse, all of which may be accompanied by limited volume surface eruptions of the lowest density melt phases. Through time, the crust-mantle boundary layer may repeatedly lift and subside through conductive heating and viscous flow, which may allow more voluminous melt migration and eruption; however, true coronae fail to develop. *INDEX TERMS:* 6295

Planetology: Solar System Objects: Venus; 5475 Planetology: Solid Surface Planets: Tectonics (8149); 8159

Tectonophysics: Rheology—crust and lithosphere; 8015 Structural Geology: Local crustal structure;

*KEYWORDS:* chasmata, coronae, mapping, tectonics, Venus

**Citation:** Bleamaster, L. F., III, and V. L. Hansen (2004), Effects of crustal heterogeneity on the morphology of chasmata, Venus, *J. Geophys. Res.*, 109, E02004, doi:10.1029/2003JE002193.

### 1. Introduction

[2] The response of a planetary lithosphere to tectonic stress is inherently dependent on its mechanical properties, which are primarily governed by the cumulative effect of its composition, thermal structure, and strain rate, which, in turn, are affected by the individual planetary body's radius, internal heat production, and heat transfer. On Earth,

lithospheric response to global stress results in a collection of linear volcanotectonic features marking the convergent and divergent boundaries of rigid plates. On Venus, despite similar physical characteristics to Earth (size, bulk composition, and internal heat budget), the present-day absence of water precludes the development of an asthenosphere [Phillips, 1986, 1990], and thus leads to very different operational mechanisms by which heat is lost. Volcanotectonic features on Venus are circular, diffuse, and distributed, much different from terrestrial focused and linear structures; however, an extensive arrangement of linear to sublinear features called chasmata, sometimes referred to as “rifts,” occur along the equatorial region of Venus (Figure 1).

<sup>1</sup>Now at Planetary Science Institute, Tucson, Arizona, USA.

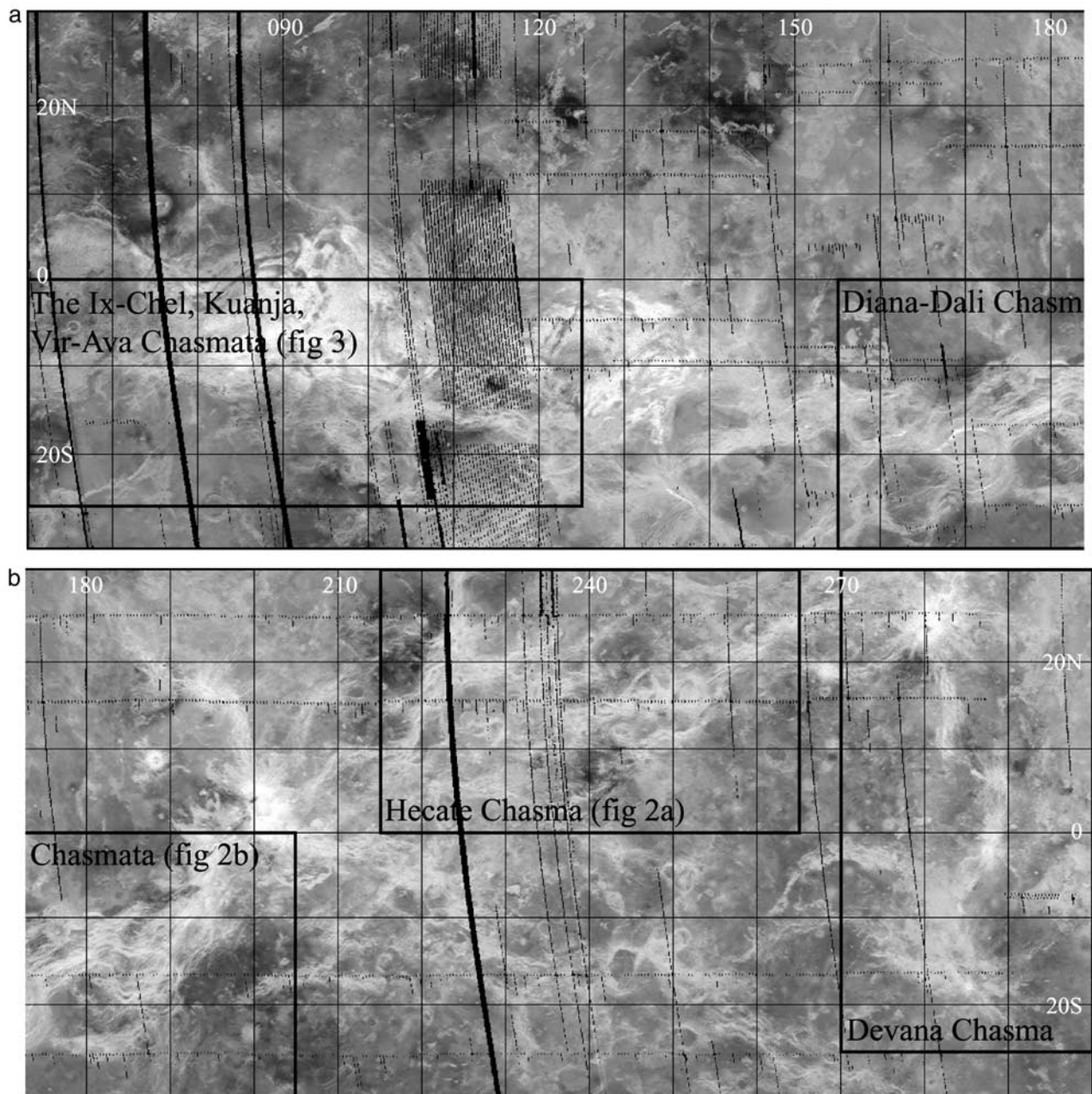


**Figure 1.** Magellan Synthetic Aperture Radar (SAR) image of equatorial region from 30°N–30°S, 060°E–300°E. Inset boxes show locations of Figures 2 and 3. Graticule at 10° intervals, Mercator projection, cycle 1.

These features and their associated deformation patterns provide clues to Venus's lithospheric rheology and operative endogenic processes. To date, arguments based on preserved large- and small-scale tectonic features across the planet have placed widely varying limits on the estimated global thickness (2 to 30 km) and the mechanical stratification (i.e., strong layer above a weak layer, or strong layer above a weak layer, above a strong layer) of Venus's elastic lithosphere [Zuber, 1987; Zuber and Parmentier, 1990; Herrick and Phillips, 1992; Grimm, 1994; Moore and Schubert, 1997]. In addition, tectonic features, coupled with geophysical analyses have been used to constrain models

that attempt to explain the general behavior of the Venusian mantle [Phillips, 1990; Solomon *et al.*, 1992; Hansen and Phillips, 1993; Hamilton and Stofan, 1996; Phillips and Hansen, 1998; Hansen, 2002, 2003; Johnson and Richards, 2003].

[3] Linear to arcuate troughs called chasmata, and circular to quasi-circular features called coronae, the foci of this work, are two specific classes of volcanotectonic features that have received much attention due to their global distribution and rich geologic histories [Baer *et al.*, 1994; Price and Suppe, 1995; Hamilton and Stofan, 1996; Copp *et al.*, 1998; Guest and Stofan, 1999; Hansen and DeShon,

2002]. Chasmata are narrow (100–200 kilometers wide, thousands of kilometers long) topographic troughs accompanied by zones of deformation and volcanism that range from 150 kilometers to over 900 kilometers in width. Pre-Magellan work initially identified approximately 20,000 linear kilometers of chasmata [Schaber, 1982]; however, increased resolution in Magellan images and altimetry expands the estimate to over 55,000 linear kilometers [Jurdy and Stefanick, 1999] (similar in length to Earth's mid-ocean spreading ridges, but much less continuous and more diffuse). Coronae [Barsukov *et al.*, 1984] ( $\geq 500$  total, median diameter 200 km [Stofan *et al.*, 1992, 2001]) are individual quasi-circular features broadly defined by an elevated annulus of tectonic structures and an interior topographic depression [Janes *et al.*, 1992; Squyres *et al.*, 1992; Stofan *et al.*, 1992]. Coronae on Venus occur in chains, clusters, or as isolated features in the plains and display a highly variable degree of surface eruption [Stofan *et al.*, 1992].

[4] Geophysical/statistical studies show that chasmata positively correlate with anomalous highs in the modeled Venusian geoid [Sandwell *et al.*, 1997; Jurdy and Stefanick, 1999], suggesting that chasmata may be forming in response to contemporary dynamic mantle activity, or upwelling. Similar types of studies attempt to relate the global population of coronae with the geoid and find that coronae exhibit neither a positive nor negative correlation with geoid anomalies [Herrick and Phillips, 1992]. The lack of spatial correlation between coronae and the geoid may illustrate a complex relationship with Venusian mantle dynamics [Hamilton and Stofan, 1996], or a temporal disconnect between the gravity field (contemporary) and a lack of constraint on the operational duration of corona forming processes (presumably globally diachronous or time transgressive) [e.g., Guest and Stofan, 1999; Chapman and Zimbelman, 1998; Johnson and Richards, 2003]. Although the global population of coronae lacks correlation with the geoid, there is a strong spatial relationship between some coronae and the global set of chasmata. Nearly 75%, or  $\sim 40,000$  linear kilometers, of chasmata display a positive spatial association with coronae [Jurdy and Stefanick, 1999]. These coronae, typically within the category of chain-forming coronae, account for 68% of the corona population [Stofan *et al.*, 1997]; thus a significantly large subset of coronae may be loosely correlated with Venus's positive geoid anomalies through their spatial associations with chasmata.

[5] This tenuous corona-chasma-geoid spatial relationship, which is bolstered by geologic mapping documenting locally complex yet nearly synchronous corona-chasma formation [Baer *et al.*, 1994; Hamilton and Stofan, 1996; Stofan *et al.*, 1997; Hansen and DeShon, 2002], lends support to the concept that chain-forming coronae and chasmata have similar genetic origins or causative relationships. Hansen and Phillips [1993] proposed, and Hamilton and Stofan [1996] and Phillips and Hansen [1998] support, that a mechanism resulting in limited lithospheric extension (either passive or active), presumably induced by coupled mantle to lithosphere tensional stresses [Phillips, 1990], is consistent with the tectonic and volcanic observations made at Hecate (Figure 2a), Diana-Dali (Figure 2b), and Parga Chasmata (each of which are significantly populated by

coronae). In contrast, the Ix-Chel, Kuanja, Vir-ava Chasmata system (IKVC) (Figure 3) and Devana Chasma ( $\sim 14,000$  linear kilometers combined) visibly lack, and are statistically anti-correlated with, coronae [Jurdy and Stefanick, 1999], despite the fact that similar mechanisms (limited extension and pressure release melting) are most likely responsible for their volcanotectonic surface expressions. Although an absence of evidence is rarely evidence of absence, the observational and statistical distinction between corona-dominated and corona-lacking chasmata raises the question, where are all of the coronae along IKVC and Devana Chasma?

[6] Because chasmata represent some of Venus's youngest features [Grimm and Phillips, 1992; Head *et al.*, 1992; Robinson and Wood, 1993; Herrick, 1994], and most have a strong correlation with coronae [Stofan *et al.*, 1997], both the formation mechanism and the mode of compensation are important for evaluating the present contribution of different heat loss mechanisms. Processes such as 1) increased heat flux and enhanced conductive cooling due to mechanical thinning of the lithosphere [Solomon and Head, 1982], 2) extrusive volcanism associated with coronae [Hansen and Phillips, 1993; Hamilton and Stofan, 1996], and 3) intrusive magmatism and underplating along chasmata, and the extent to which each of these processes operate, become crucial for unraveling Venus's thermal state and history. Evaluation of the spatial distribution, geomorphology, and geologic history of the major chasma segments and coronae also yields useful information about mantle-lithosphere interactions [Stofan *et al.*, 1997] and local assessments may carry global implications. Therefore detailed investigations into the process(es) responsible for interrelated chasma-corona formation and the local environmental factors (i.e., thermal regime, crust-lithosphere properties) that affect the surface morphology of these features are needed.

[7] The following work consists of a detailed geologic-morphologic-structural evaluation of the IKVC system. We propose a diapir stagnation model that suggests laterally variable crustal differences (mechanical and chemical) are responsible for influencing the surface manifestation of corona-forming diapirs, thus affecting the morphology of chasmata across the planet (specifically the presence or lack of coronae). Chasma deformation is accompanied by corona development when forming in regions of nominal crust, typified by plains-type crust, but lack corona features when influenced by crustal heterogeneities at depth associated with thick crustal plateau roots (i.e., Ovda and Phoebe regions). These results support the idea that chasmata, despite having highly variable surface characteristics, represent a common dynamic process and are responsible for significant upward mobilization of material and heat from the mantle to the surface, but different modes of material transport result depending on the existing local lithospheric/crustal environment.

## 2. Geologic Setting and Mapping

[8] The Ix Chel, Kuanja, and Vir-ava Chasmata (IKVC) collectively define a geographic and geomorphic division between Aphrodite Terra and Aino Planitia (Figure 3). Nearly 7000 kilometers in length, the IKVC separates the highstanding crustal plateau terrain of western, central, and

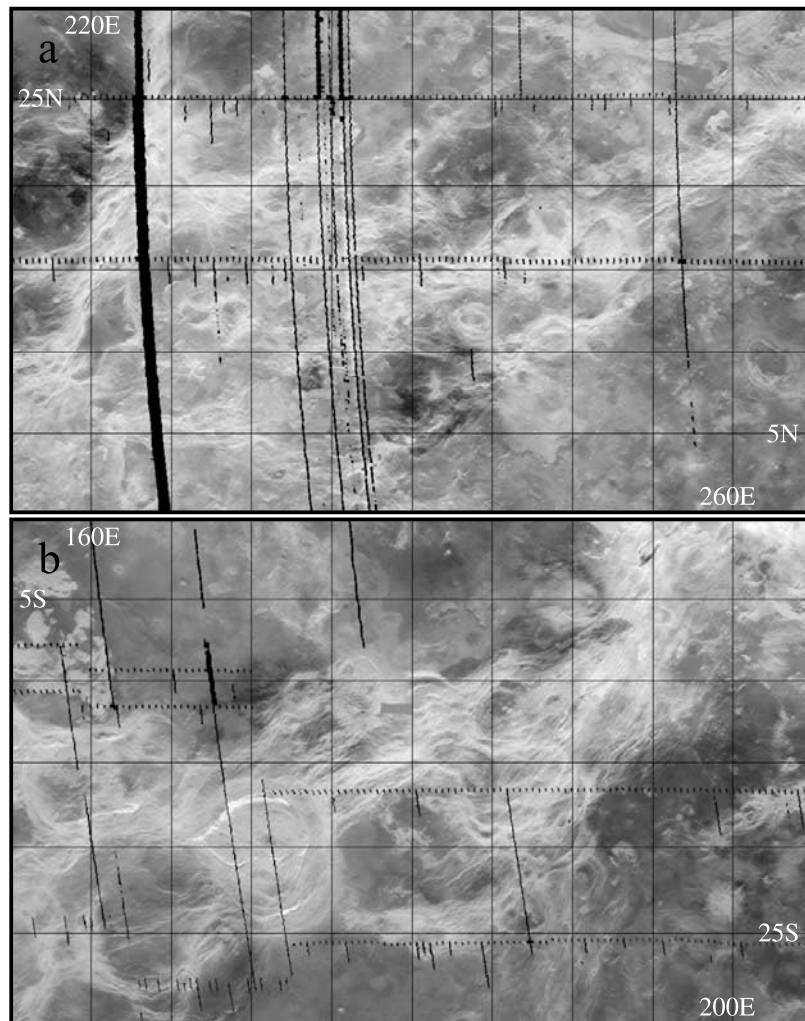


**Figure 2.** (a) Hecate Chasma (upper left corner at  $30^{\circ}\text{N}$ ,  $215^{\circ}\text{E}$ ) and b) Diana-Dali Chasma (upper left corner at  $0^{\circ}\text{N}$ ,  $155^{\circ}\text{E}$ ) both visually and statistically exhibit a strong spatial correlation with coronae features. Coronae-chasmata, volcanotectonic relationships observed in these regions support the hypothesis that they are zones of limited lithospheric extension accompanied by diapiric rise that results in coronae [Hansen and Phillips, 1993; Hamilton and Stofan, 1996]. Graticule at  $5^{\circ}$  intervals.

eastern Onda Regio and Thetis Regio from the lower lying southern “plains.” Broadly defined by its east-west trending trough, the IKVC includes three major discontinuous trough segments with consistent floor depths 1–1.5 kilometers below mean planetary radius (6051.8 km). Structural relief (flank to floor height) varies between 1.5 to 4 kilometers. Additionally, trough segments are marked by numerous linear to arcuate structural suites. The combination of topographic troughs and deformation suites define the complete IKVC zone (from  $0^{\circ}\text{N}$ ,  $060^{\circ}\text{E}$  to  $15^{\circ}\text{S}$ ,  $130^{\circ}\text{E}$ ). Although the structural suites are broadly undulatory and locally anastomosing, the IKVC topography contains two distinct (one major and one minor) en echelon offsets between  $085^{\circ}\text{E}$ – $090^{\circ}\text{E}$  and  $103^{\circ}\text{E}$ – $108^{\circ}\text{E}$ . Each offset marks a significant geomorphic change, potentially reflecting unique structural development along the IKVC.

[9] Detailed structural mapping, utilizing the highest resolution Magellan synthetic aperture radar (SAR) and altimetry data, has expanded and enhanced regional 1:5,000,000 scale geologic mapping of the Kuanja and

Vir-ava Chasmata [Bleamaster and Hansen, 2004]. Following is an explanation of the volcanic and tectonic features preserved along various tracks of the IKVC system starting in the west and progressing east.

### 2.1. Ix-Chel Chasma

[10] Verdandi Corona (Figure 4a), located centrally in western Onda Regio, marks the most westerly extent of the Ix-Chel segment. Although a well-formed circular corona, Verdandi displays some structural asymmetry. The eastern margin is dominated by an arcuate band of lineaments, characterized by gradational radar tonality, whereas the western margin displays both arcuate and linear sets of lineaments with sharp radar contrast margins. Verdandi structures deform radar-dark flow materials that may either represent flows from the initial volcanic stages associated with corona formation, or preexisting volcanic flows that flooded topographic lows within the crustal plateau interior. Without primary flow features, or identifiable volcanic vents within the radar-dark material, it is difficult to

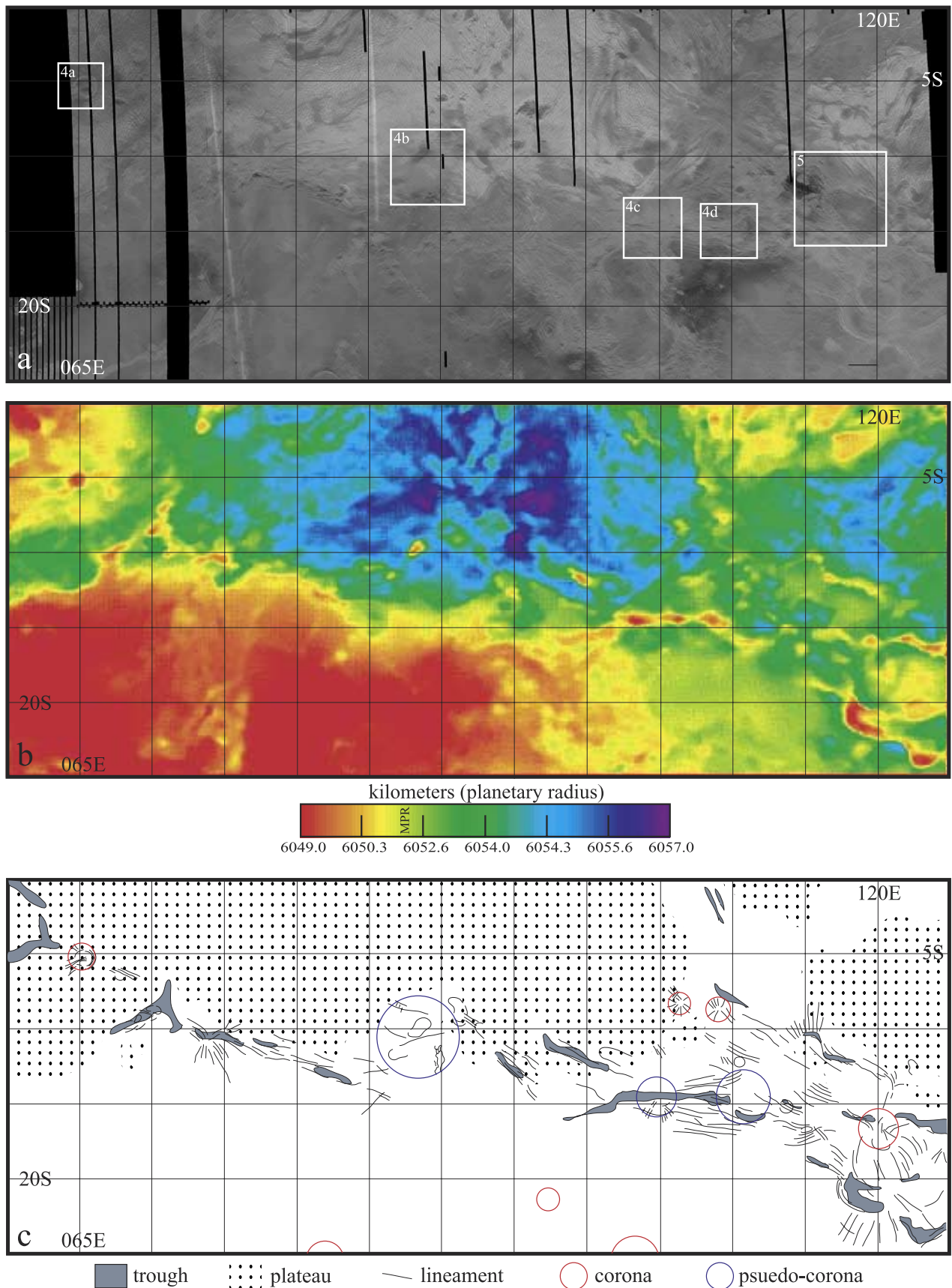


**Figure 3.** (a) Right-look SAR, (b) altimetry, and (c) schematic map of the Ix-Chel, Kuanja, Vir-ava chasmata and surrounding area. Inset boxes locate other figures.

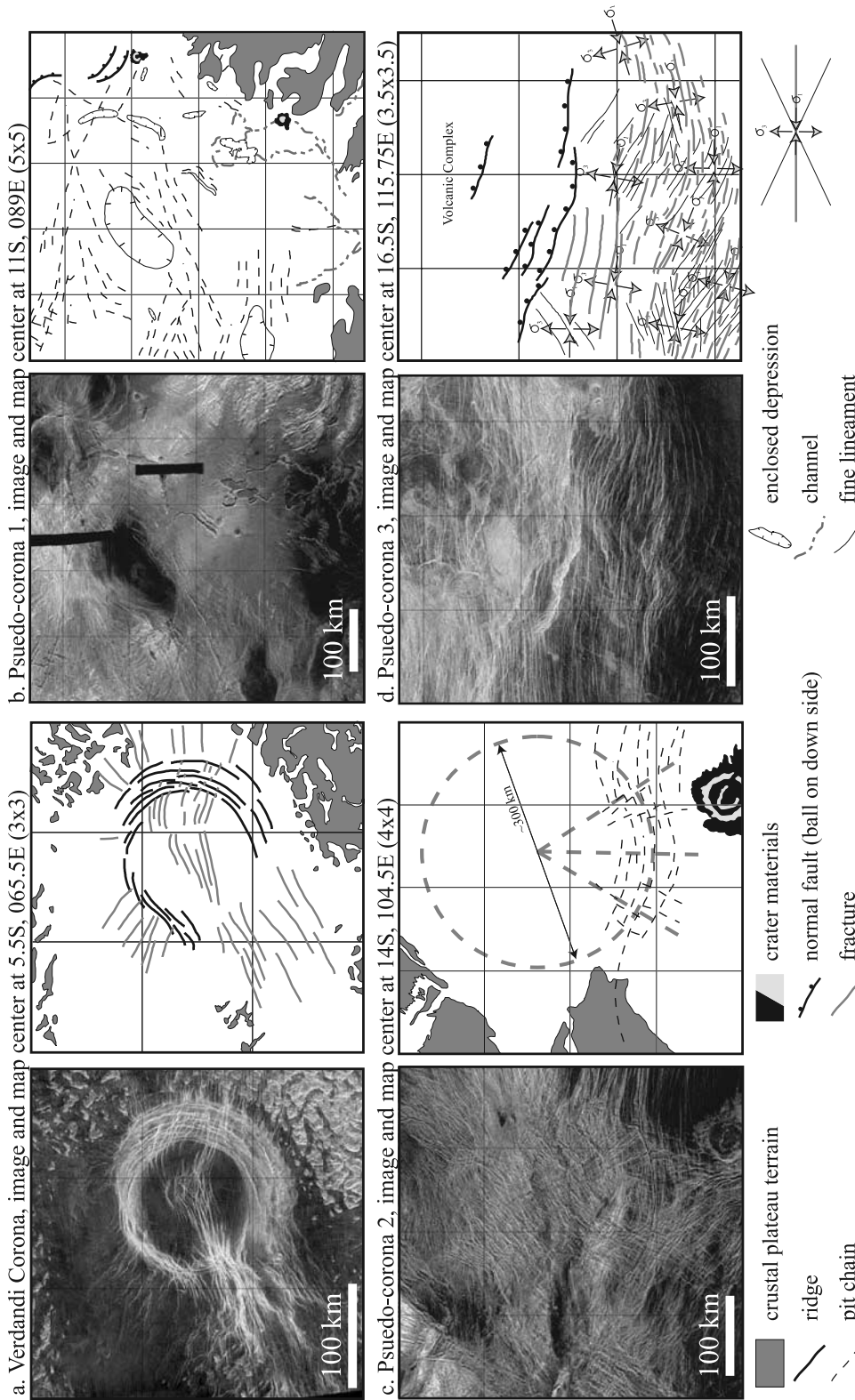


**Figure 4.** SAR images and corresponding sketch maps of four circular to semicircular volcanotectonic features along IKVC. (a) Verdandi Corona, centrally located within western Ovda Regio, represents the western-most extent of the Ix-Chel Chasma. (b) Ovoid depression, pit chains, and lava channels along the southern portion of Ovda Regio. This area marks the transition from the Ix-Chel Chasma to the east to the Kuanja Chasma to the west. Regional doming and associated tectonic structures are presumed to have formed in response to plume [Baker *et al.*, 1997] or diapir ascension; however, the lack of coherent patterns may be evidence of diapir impedance within the thick crust of Ovda. (c) Southeastern boundary of Ovda Regio. Pit chains display both circumferential and radial components; extrapolation of these trends is illustrated by the dashed lines and shows the potential diameter and center of a fully developed volcanotectonic center. (d) The systematic relationship that exists among cross fractures, open mode fractures, and principal stress directions provide a basis for interpreting the paleostress directions. In a purely north-south extensional regime, sigma one would be oriented east-west. Above, the principle stress indicators illustrate an arcuate component to the paleostress orientations resulting from local perturbations of the regional stress field. These perturbations may be the result of the introduction of a significant volcanic load to the north. Graticule at 1° intervals.

determine the source of the volcanic materials; however, the arcuate embayment of the crustal plateau terrain along the eastern margin of Verdandi suggests that volcanic flows and deformation may be genetically related. The morphology and distribution of the structural suites and the surrounding flow deposits of Verdandi are consistent with existing models for corona formation [Squyres *et al.*, 1992], with the eastern margin (interpreted to represent an arcuate fold belt because of the gradational radar tonal changes across their culmination) and western margin (dominated by east-trending fractures) forming in response to doming above, and lateral spreading of, a diapir as it impinged against a zone of neutral buoyancy.

[11] López [2002] proposed that lithospheric variability, resulting from preexisting thermal or structural heterogeneities, influences the surface morphology of coronae (specifically multicoronae). Verdandi's structural asymmetry may indicate some degree of heterogeneity, or anisotropy of the mechanical properties of the elastic lithosphere during corona formation. Small- or regional-scale crustal and/or lithospheric topological differences may have influenced the subsurface flow of the corona-forming diapir, and therefore affected the structural style and orientation of features across the corona. For example, the corona eastern margin (fold belt) may be the result of local buttressing by the crustal plateau terrain to the east; whereas the western edge (east-trending fractures) may have been influenced by regional stresses related to overall north-south extension.

[12] Ix-Chel Chasma trends southeast from Verdandi, where it encounters and then follows the southern most margin of central Ovda Regio. Topographically, Ix-Chel Chasma is the narrowest and shallowest portion of the IKVC. Difficulties arise when attempting to define the Ix-Chel Chasma because of its close proximity to both the highland plateau region to the north and the plains to the south. The northern flank sits well above ( $\sim 2$  km) the southern flank, within the crustal plateau terrain of central Ovda Regio. The southern flank slopes gradually into Aino Planitia, the southern plains region. Although poorly defined topographically, and sparsely populated by tectonic lineaments, the Ix-Chel segment is generally straight for nearly 1500 kilometers and shows progressive increases in both depth and structural development to the east, which is consistent with the inference that the rift is propagating, or unzipping, to the west [Bleamaster and Hansen, 2004; M. S. Gilmore, personal communication, 2001].

[13] Ix-Chel Chasma terminates to the east at  $085^\circ\text{E}$ , marking a distinct transition in chasm morphology (from continuous, focused, and straight to discontinuous, distributed, and arcuate). Here, a set of northeast-trending elongate ovoid depressions (Figure 4b) marks the first, and larger of the two, en echelon offsets of the main topographic trough. The region also marks a change from a tectonically to a volcanically dominated area. The immediate area contains fewer linear structural sets; however, some concentric normal faults, pit chains and troughs surround the ovoid depressions. Although devoid of large volcanic constructs and associated major radial/concentric structure sets, the entire region is domed upward ( $<1$  km) with a centrally located large ( $\sim 150$  km diameter) caldera-like depression. To the south, two smaller calderas and numerous sinuous

“canali” feed the flows of LoShen Valles ( $12^\circ\text{S}$ ,  $089^\circ\text{E}$ ) [Bleamaster and Hansen, 2004]. Baker *et al.* [1997] attributed the volcanic, tectonic, and channel-forming activities in this locality to volcanism and tectonism resulting from mantle plume activity. This area could also represent a more local, shallowly derived diapiric body spawned from a broad upwelling with the flows forming in response to melting associated with the introduction of heat and/or material convectively supplied to the upper mantle. Low-density melt phases could percolate up through the crust of southern Ovda by way of fractures/dikes, open conduits, and magma chambers. In this scenario the tectonic structures and calderas may reflect vertical motions of the elastic lithosphere with collapse related to magma migration and evacuation.

## 2.2. Kuanja Chasma

[14] Kuanja Chasma continues east of the transition zone beginning near  $10^\circ\text{S}$ ,  $095^\circ\text{E}$ . Kuanja consists of two parallel troughs flanked on either side by crustal plateau terrain of eastern Ovda Regio. The northern trough, wider and deeper than the south trough, consists of numerous parallel graben and half-graben. Kuanja trends southeast and eventually joins the Vir-ava segment at the deepest point along the IKVC ( $14^\circ\text{S}$ ,  $103.5^\circ\text{E}$ ). This junction marks the first of two prominent semicircular structural sets that lie along IKVC, which is characterized by predominately linear structures. The first structural set ( $14^\circ\text{S}$ ,  $105^\circ\text{E}$ ) (Figure 4c) consists of a partially radial, and a partially concentric, suite. The radial structures sweep out an approximately  $60^\circ$  arc that trends from the southwest to the southeast. Each radial lineament is  $\sim 25$  to 50 kilometers long and a few 100 meters to a few kilometers wide. Many lineaments display a scalloped margin typical of structures within the IKVC [Bleamaster and Hansen, 2001]. The concentric suite is made up of dozens of fine lineaments and one major scalloped trough. Most of the fine lineaments are 50 to  $\sim 200$  kilometers long and arcuate in planform shape; however, the major scalloped trough is over 500 kilometers long and transitions from straight to arcuate along its length. The arcuate portion of this trough is orthogonal to the radial structures. Although this pattern does not describe a full circle, extrapolation of the arc and elongation of the radial components places the center of deformation in the same location and near the center of the chasmata track (Figure 4c).

## 2.3. Vir-ava Chasma

[15] Continuing east into Vir-ava Chasma, the rift morphology changes, becoming wider, more diffuse, and a more constant depth. Vir-ava Chasma, although near crustal plateau terrain, does not intersect either Ovda Regio or Thetis Regio and displays morphology more similar to that of Diana-Dali, Parga, and Hecate Chasmata; however, Vir-ava Chasma does not display any prominent corona features.

[16] A second semicircular structure set ( $17^\circ\text{S}$ ,  $111.5^\circ\text{E}$ ), containing three lineament suites, occurs near the center of Vir-ava Chasma. Two of the three lineament suites contain very fine lineaments that are only one or two pixel elements across even in the highest resolution SAR, making identification of the specific structural elements difficult.

Turan Planum, image and map center at 13S, 117.5E (6.5x6.5)

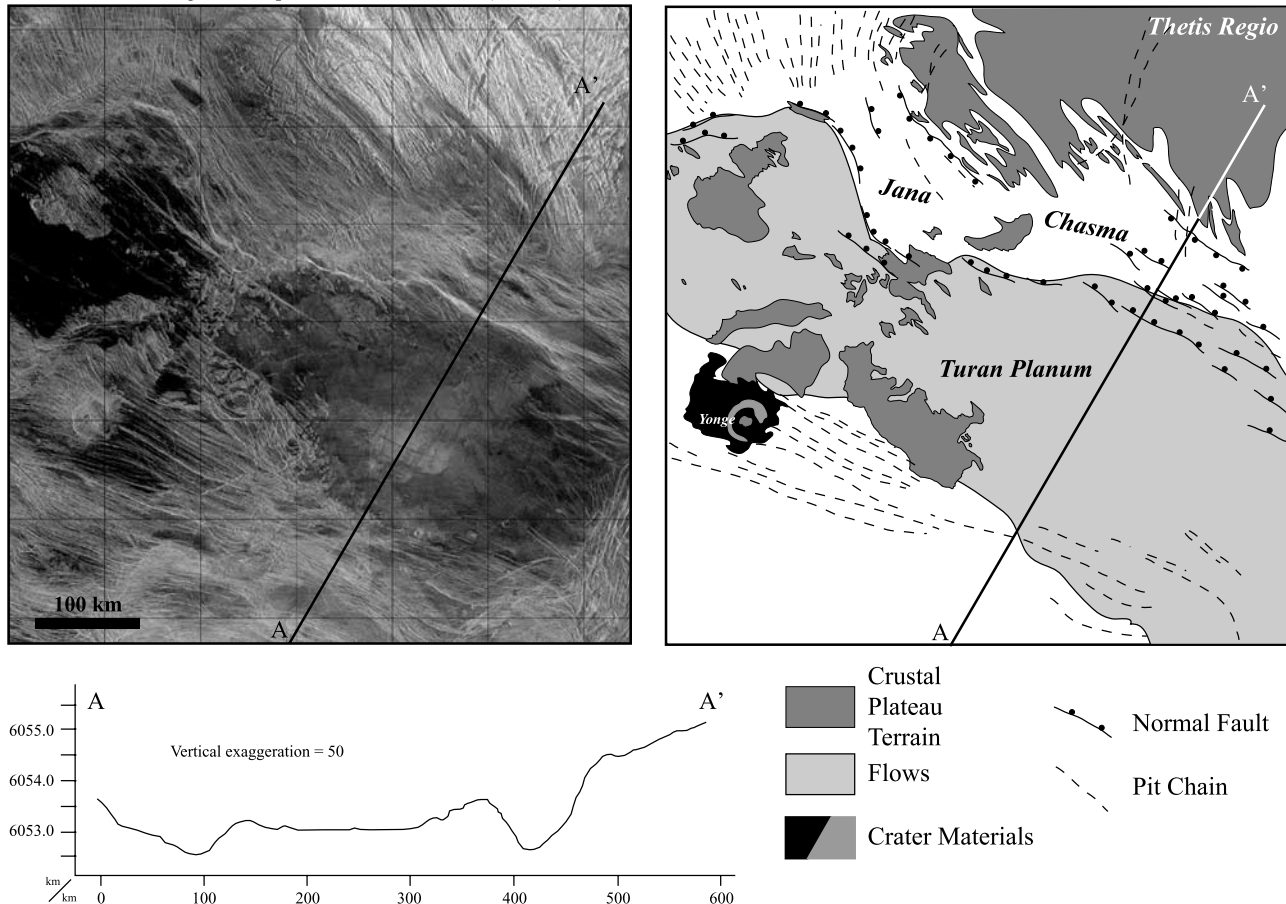


**Figure 5.** SAR image and sketch map of the Turan Planum and Jana Chasma. Topographic profile across A-A' illustrates topographic-lithologic correlation as well as relief across the chasma. An estimate of extension across the Jana Chasma is approximately 2.5 km.

However, the two suites can be differentiated by orientation; one suite trends predominantly northeast and the other predominantly southeast. An internal angle of 30–40° between the suites is locally consistent. The third structure suite contains features that are significantly wider and shorter than suites one and two. Each individual structure in the third suite is a paired lineament, which is interpreted to represent two edge reflectors bounding a topographically low center. This radar configuration has been interpreted to represent either a graben or tensile fracture depending on the type of fracture termination (ramp or v-shape [Hansen and Willis, 1996]). The structures within the third suite are too fine to make the distinction between graben and tensile fractures; however, because each morphology (graben or tensile fracture) represents extension this structure suite can be satisfied by either a mode 1 opening fracture or paired mode 3 shear fracture hypothesis [Atkinson, 1987; Engelder, 1987]. Orientation of the third suite gradually changes trend from southeast to east to northeast (as traversed from west to east).

[17] Together the three structural suites define a consistent bulk strain pattern containing 1) an arcuate set of cross fractures [Willis and Hansen, 1996] (suites 1 and 2), and 2) extension fractures that consistently bisect the acute angle of the cross set (suite 3) (Figure 4d). The first two suites,

interpreted as cross-fractures, cannot be proven to have formed synchronously (therefore conjugate); however, the systematic geometric relationship that exists between the cross fractures and the third suite of structures is consistent with the paleostress orientations during their formation and argues against a serendipitous geometric pattern. Consistent with bulk strain analysis, the direction of greatest principal stress ( $\sigma_1$ ) bisects the acute angle of the cross fractures and is parallel to the extension fractures (suite 3). Like the first semicircular structural set, this set creates a partial circular pattern with an extrapolated circle center lying along the main chasma track. The Kuanja and Vir-ava structural sets occur only on the southern flank of the chasma, indicating that they either 1) only formed on the southern flank or 2) were only preserved there.

#### 2.4. Turan Planum

[18] Nearing the eastern extent of IKVC is Turan Planum. Turan Planum is a moderately flat volcanic field surrounded by an elevated margin with penetrative chasmata and coronae structures outboard of its rim (Figure 5); Jana Chasma lies to the north, Vir-ava Chasma to the south, and Inari Corona to the southeast.

[19] Jana Chasma, located along the southern boundary of Thetis Regio north of Turan, is characterized by a series of

east-striking normal faults. Thetis Regio, a 4 kilometer-high crustal plateau, displays a coherent set of intersecting lineaments referred to as tessera terrain [Barsukov *et al.*, 1986]. The tessera terrain is thought to represent coherent deformation and is capable of preserving consistent bulk strain patterns over vast regions [Hansen and Willis, 1996, 1998; Ghent and Hansen, 1999; Hansen *et al.*, 1999, 2000; Bleamaster and Hansen, 2004]. Within Turan Planum (12°S, 115°E), a moderately highstanding flooded plateau, sit numerous small outcrops of tessera with structural trends similar to the overall pattern preserved in Thetis Regio. On the basis of the consistent tessera structural trends of the tessera on either side of Jana Chasma, it is suggested that the tessera within Turan Planum and Thetis Regio were once contiguous terrain [Bleamaster and Hansen, 2004]. A genetically linked origin is also supported by the preserved high elevation of Turan Planum, which may indicate that it is supported by thickened crust, similar to Thetis Regio [Grimm, 1994; Simons *et al.*, 1997]. It is envisioned that normal faulting, representing general north-south extension, served to separate a portion of tessera terrain from the main crustal plateau. Although the true amount of strain cannot be determined because we lack the ability to determine predeformation lengths, cumulative extension across Jana Chasma can be estimated using simple trigonometry.

$$\text{Extension} = h / \tan(\emptyset) \quad (1)$$

Assuming an estimated fault dip,  $\emptyset$ , here taken as 60°, consistent with rock failure criteria for vertically oriented maximum stress (gravity) [Anderson, 1951], and  $h$  as the sum of total flank to trough height difference from both sides of the trough results in ~2.5 km extension across Jana Chasma. Although this represents minor deformation, Jana Chasma is a secondary branch of the main IKVC system and does not represent the extension accommodated by all four chasma segments. The estimated value also underestimates the amount of extension because volcanic flows and debris infilling have not been accounted for, which would serve to decrease the total flank to floor height. Only if the fault dips are significantly greater than 60° will estimated cumulative extension be an over estimate.

[20] Flows from various sources, including Inari Corona, flood the isolated plateau. The Turan Planum floor is relatively smooth and contains only a few east-trending chasma structures (pit chains and volcanic fissures). It is envisioned that structural isolation of Turan Planum (fault bound block) may have led to strain partitioning around the plateau, much like ductile fabrics wrap around strong porphyroclasts in terrestrial metamorphic rocks.

[21] The different features along the chasma illustrate that both extension and volcanism were important processes in the formation of the IKVC. Several volcanic regions (each ~150–500 kilometers in diameter), from the well-formed Verdandi Corona to the less recognizable volcanic constructs (pseudocoronae) (Figure 4), indicate that there are locally significant regions of magma production along the IKVC. Structural elements along IKVC are also consistent with development of local point source loads that have affected the regional stress field, causing circular to semicircular structural sets. The combination of volcanic and structural evidence leads to a hypothesis that intrusive and extrusive

magmatism spawned from diapirs associated with broad upwelling (as indicated by the geoid) have stalled beneath or within moderately thickened crust associated with crustal plateau terrain. Diapir stagnation results in various types of surface manifestation of rising mantle diapirs, perhaps including pseudocoronae. The following section will highlight our current understanding of corona and chasma formation before introducing the diapir stagnation model.

### 3. Corona/Chasma Background

[22] Chain-forming corona and chasmata are predominantly located within the equatorial region of Venus and nearly completely encircle the planet (Figure 1). Together, they also characterize much of the mesoland (around mean planetary radius) topography, which is distinct from the rolling plains and lowlands (~70% of Venus's surface), and the highlands consisting of crustal plateaus, volcanic rises, and Ishtar Terra. Geophysical modeling (theoretical, geodynamic, and gravity-topography relations) places constraints on the modes of formation responsible for, and compensation of, most of Venus's topographic variations. It is currently believed that the plains' low topography reflects present-day, broad downwelling [Herrick and Phillips, 1992; Rosenblatt and Pinet, 1994], whereas crustal plateaus (isostatically supported on short time-scales) and volcanic rises (dynamically supported) represent the surface expressions of deep mantle plumes on an ancient thin [Hansen *et al.*, 1997, 1999; Hansen and Willis, 1998; Phillips and Hansen, 1998] and a contemporary thick [McGill *et al.*, 1981; Phillips and Malin, 1984; Smrekar *et al.*, 1997] lithosphere, respectively. Ishtar Terra results from a combination of early crustal plateau processes, subsequently caught in an ancient broad downwelling; Ishtar's extreme topography is presently supported by accumulated mantle melt residuum [Hansen and Phillips, 1995]. Compensation of mesoland topography (including corona and chasmata) may be characterized, depending on the preferred model of formation, as isostatic (including compositional differences and/or crustal thickness variations), dynamic (by means of thermal expansion related to upwelling and thinning of the thermal lithosphere), or a combination of these factors.

#### 3.1. Corona Formation

[23] To date, much research has focused on corona (as reviewed by Stofan *et al.* [1997]), and has been concerned with 1) classification, 2) morphological differences [e.g., Stofan *et al.*, 1992; Hamilton and Stofan, 1996; DeLaughter and Jurdy, 1999], 3) spatial distributions [e.g., Jurdy and Stefanick, 1999; DeLaughter and Jurdy, 1999], 4) implications of temporal significance [e.g., Chapman and Zimbelman, 1998; DeLaughter and Jurdy, 1999], and 5) corona evolution [e.g., Squyres *et al.*, 1992; Stofan *et al.*, 1992]. Workers have also surveyed corona within volcanic rises [Smrekar and Stofan, 1999], and some corona-dominated chasmata, including 128 corona along Parga Chasma [Stofan *et al.*, 2000] and 46 along Hecate Chasma [Hamilton and Stofan, 1996].

[24] Corona are quite complex in detail, displaying a multitude of morphologies (see classification of Stofan *et al.* [1997]); however, in general they are circular to quasi-circular features characterized by a topographically elevated

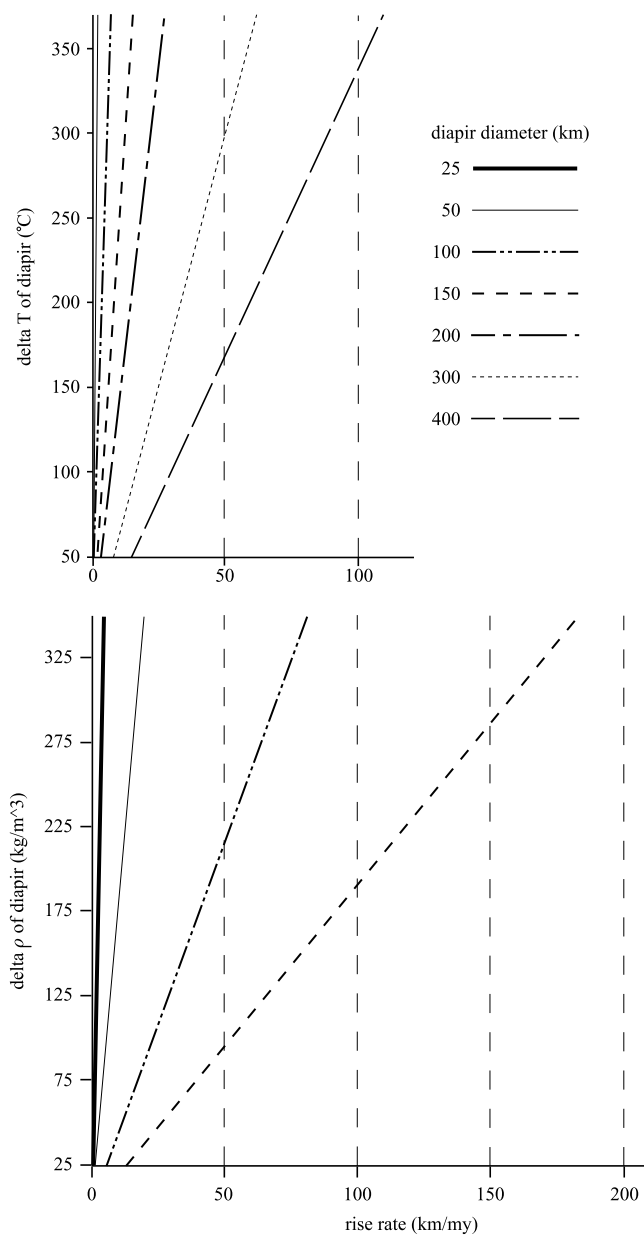


**Figure 6.** Rates of rise for thermal (top) and compositional (bottom) diapirs as a function of diapir diameter [Hansen, 2003]. Note that a 150 km diapir will rise at the same rate with the maximum  $\Delta T$  (temperature-dependent density difference) and the minimum  $\Delta \rho$  (compositionally dependent density difference) values evaluated. Calculations do not consider cooling of the diapir, which would actually slow the diapir's rate of rise through time.

annulus of concentric structures (both extensional and contractional), radiating fractures, and varying amounts of volcanic flows [Janes *et al.*, 1992; Squyres *et al.*, 1992; Stofan *et al.*, 1992]. Principal stages in the general conceptual model of corona formation include the following: 1) a diapir rises through the mantle toward the surface forcing domical uplift of the lithosphere that is accompanied by radial fracturing and volcanism, 2) as the diapir impinges on the base of the lithosphere, causing spreading

and flattening, the shape of the uplift transforms from domical to plateau-like while volcanism may or may not continue, and 3) diapir cooling removes thermal topographic support, allowing gravitational relaxation to form a moat, rim, and interior depression which may be accompanied by concentric fracturing [Squyres *et al.*, 1992; Stofan *et al.*, 1992, 1997]. Although never explicitly stated, the conceptual model appears to assume that the rising diapirs are driven by thermally derived density contrasts. This is supported by statements from the model that envisage corona features forming when 1) a diapir stalls at the lithospheric boundary (a mechanical boundary established by the local thermal environment either representing a transition from convective to conductive heat transfer (thermal lithosphere), or from ductile to brittle behavior of the rock (elastic lithosphere)), and 2) the central topography collapses because of a loss of dynamic support in response to conductive cooling.

[25] In contrast to a thermal origin for coronae, Hansen and Phillips [1993] proposed that the coronae within the eastern Aphrodite Terra chasmata region are formed by magma diapirs derived from the upper mantle as buoyantly unstable partial melts. As demonstrated by Griffiths [1986], diapirs with buoyancy driven by compositional differences (including melt or partial melts; physical and/or chemical phase transformations) rise and evolve differently from thermal (buoyancy due to temperature difference only) diapirs. Application of these concepts to corona diapirs indicates that corona-forming diapirs likely result from compositional, rather than thermal diapirs [Hansen, 2003]. By calculating the average rise-times of various sized Venusian diapirs with either temperature- or compositionally-dependent density contrasts, Hansen [2003] displays the inability of small-sized, thermally buoyant diapirs (like those proposed in current corona models) to traverse the upper mantle and reach the surface prior to cooling; alternatively, small compositionally buoyant diapirs maintain their buoyancy (and rise rates) and may ascend further through their surrounding medium (Figure 6). Conversely, large thermally buoyant plumes spawned from the core mantle boundary can maintain elevated temperature differences from the surrounding mantle and may traverse the mantle. Dombard *et al.* [2002], although circumventing the thermal versus compositional argument for various-sized diapir-related phenomena, also recognized the validity of compositionally derived components (partial melts) for corona formation. Thus it seems legitimate to entertain the possibility of compositionally derived diapirs.

[26] Consequently, the previously described conceptual (thermal) model for corona formation (phases 1–3) requires slight modification to satisfy a compositional diapir formation mechanism. In general, the premise remains the same, a buoyantly unstable diapir rises through the mantle until it reaches an area of neutral buoyancy; for a compositional diapir this would be either at the base of the crust or somewhere within the crust. The late stage interior collapse, attributed to thermal decay in the previous model, may in fact be due to the evacuation of the lowest density partial melts from near-surface magma chambers. In any case, all viable mechanisms (thermal, compositional, or both) must be considered when attempting to discern the process(es)

and environments that may affect the spatial distribution of coronae.

### 3.2. Chasmata Formation

[27] Chasmata on Venus occur within a variety of geographic and geologic settings. They have been postulated (not collectively, but at various locations) to be everything from divergent zones, spreading centers, and continental rifts [Phillips *et al.*, 1981; McGill *et al.*, 1981; Head and Crumpler, 1987; Stofan *et al.*, 1989; Solomon *et al.*, 1992; Suppe and Connors, 1992; Rathbun *et al.*, 1999] to sites of convergence or subduction, and even lateral shear [Sandwell and Schubert, 1992; McKenzie *et al.*, 1992; Brown and Grimm, 1995; Schubert and Sandwell, 1995]. With the exception of Artemis Chasma, which likely results from the interaction of a mantle plume (the chasma itself not being the entire manifestation of the mantle plume) with the lithosphere [Hansen, 2002], a preponderance of extensional structures and associated volcanic features is leading to a broad consensus that chasmata represent zones of limited lithospheric extension accompanied by various degrees of magma production [Stofan *et al.*, 1992; Hansen and Phillips, 1993; Hamilton and Stofan, 1996; Stofan *et al.*, 1997; Bleamaster and Hansen, 2001]. Although previous studies have recognized chasma sections that lack coronae [Jurdy and Stefanick, 1999; Jurdy and Stoddard, 2001], a comprehensive comparative morphological analysis of chasmata from the various physiographic regions (i.e., chasmata within plains versus chasmata near crustal plateaus) is absent from the literature.

[28] Geologic and structural mapping has documented synchronous chasmata-coronae formation along many major chasma segments [Baer *et al.*, 1994; Hamilton and Stofan, 1996; Stofan *et al.*, 1997]; however, these observations do not hold for chasmata that show evidence of significant tectonic and volcanic activity yet lack coronae. The lack of corona features suggest that either 1) diapirs at depth never form, therefore precluding the development of coronae, or 2) the diapirs form, yet never impart a surface signature in the form of coronae. The four previously described 150–500 km diameter volcanic complexes and pseudocoronae (semicircular volcanotectonic forms) along the IKVC lend support to the later hypothesis. The spatial and temporal relationships of the forms are consistent with the overall conceptual model of chasma (extension)-corona (diapir) formation, but their failure to fully form suggests that a mechanism may prohibit, and thus affect the surface manifestation of, these corona-forming diapirs. The following section will outline the specifics of the diapir stagnation model including discussion of neutral buoyancy and mechanical strength.

## 4. Diapir Stagnation

[29] Crustal plateaus are highstanding, steep-sided, flat-topped, quasi-circular regions characterized by ribbon-bearing tessera fabrics [Bindschadler *et al.*, 1992a, 1992b; Phillips and Hansen, 1994; Hansen and Willis, 1998]. Their gravity-topography signatures exhibit signs of being shallowly compensated and isostatic over short timescales. Both Pratt (compositional contrast) and Airy (thickness contrast) compensation models can be constructed to fit

their observed gravity signatures. However, considering that Venus lacks appreciable water and plate tectonic processes [Solomon, 1993] (circumstances that facilitate the generation and preservation of large tracks of low density ( $\sim 2.7 \text{ g cm}^{-3}$ ), continental-type crust), it is more probable that Airy-type compensation, indicative of locally thickened crust of similar composition to the surrounding lower lying areas, is responsible for crustal plateau support [Herrick *et al.*, 1989; Smrekar and Phillips, 1991; Bindschadler *et al.*, 1992a; Herrick and Phillips, 1992; Grimm, 1994; Simons *et al.*, 1994, 1997]. Crustal thicknesses within crustal plateaus range from 35 to 80 km, which is 2 to 4 times the thickness of the surrounding plains (estimated between 20 and 50 km [Grimm, 1994; Grimm and Hess, 1997; Moore and Schubert, 1997]). The consequence of locally thickening the crust, which increases the depth of the chemical boundary between the crust and mantle, laterally affects both the vertical density profile and the mechanical strength of the outermost layer on Venus (Figure 7). The combination of increasing the depth to neutral buoyancy and mechanical weakening at depth (below the brittle regime) would decrease the ability for mantle diapirs to impart a surface corona signature by effectively producing both a density trap and a weak lower crust (ductile strain magnet).

[30] Despite controversy concerning the formation mechanism of tessera terrain and crustal plateaus [e.g., Bindschadler *et al.*, 1992a; Bindschadler, 1995; Gilmore *et al.*, 1997, 1998; Hansen and Willis, 1998; Hansen *et al.*, 1997, 1999, 2000, and references therein], ideas presented in this work are independent of the process(es) responsible for crustal thickening.

### 4.1. Neutral Buoyancy

[31] Crustal plateaus, formed by either deep-mantle plumes, resulting in a combination of volcanic extrusion, magmatic intrusion, and underplating [e.g., Phillips and Hansen, 1994, 1998; Hansen *et al.*, 1997, 1999, 2000; Hansen and Willis, 1998], or by large-scale contraction and underthrusting resulting in an approximate doubling of nominal crustal thickness [e.g., Bindschadler *et al.*, 1992a, 1992b; Bindschadler, 1995], represent secondary basaltic composition crust, the result of partial melting of the mantle. Remelting of basaltic material may result in increased differentiation and the creation of tertiary crust (more felsic); however, there are only a few examples of potentially siliceous flows and little evidence for widespread remelting. Although the density structure of the Venusian crust remains unknown, it may be approximated as having a similar surface density to that of subaerial basalt ( $\sim 2.8 \text{ g cm}^{-3}$ ) and increasing density with depth as a result of pore space compaction ( $\sim 2.9\text{--}3.1 \text{ g cm}^{-3}$ ) [Head and Wilson, 1992]. Therefore material derived from the mantle through the process of partial melting will have compositions similar to the bulk of the crust, and will maintain densities less than that of the mantle and similar to that of the overlying crust [Grimm and Hess, 1997].

[32] Koch and Manga [1996] evaluated the topographic effect rising mantle diapirs have on the surface. They used diapir-mantle density contrasts equal to  $100 \text{ kg m}^{-3}$ , and crustal thickness (b) to diapir radii (a) ratios of 0.05 to 0.5 [Koch and Manga, 1996, Figure 2]. Considering a mean

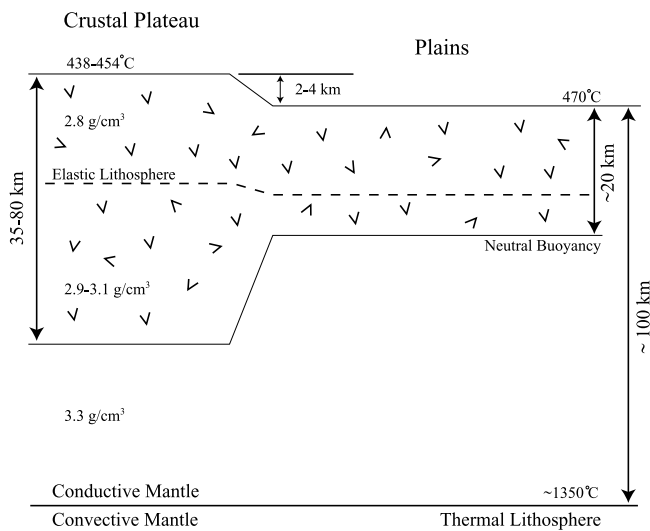


**Figure 7.** Schematic representation of various physical characteristics of crustal plateaus and plains regions. Crustal thickness differences between crustal plateaus (thick crust) and plains (nominal crust) result in drastically different 1) depth to neutral buoyancy, and 2) mechanical strength of the lower crust.

size corona of 200 km diameter [e.g., *Stofan et al.*, 1992], and a 2 to 1 corona- to diapir-diameter flattening ratio [*Whitehead and Luther*, 1975] (diapir radius equals 50 km), the crustal thickness would need to be much less than 20 km for significant coronae development to occur. For crust thicker than 20 km ( $b/a > 0.4$ ), the diapir remains too deep to produce significant topographic relief [*Koch and Manga*, 1996]. Even in the case of a moderately large corona (350 km diameter), crustal thickness values must be less than 35 km in order to produce a topographic signature.

[33] Therefore, in regions characterized by relatively thin crust (<20 km), like the plains, shallow neutral buoyancy zones could develop, diapirs could rise to the base of the crust, begin to flatten, and impart a surface signature containing both the surface structures and topographic signature characteristic of coronae. Alternatively, a thick crust (>40km) increases the depth to the neutral buoyancy zone and diapirs would be halted at depths that would inhibit corona formation (Figure 8). If Koch and Manga's analysis holds true, it implies that wherever coronae develop, the crustal thickness must be less than 0.1 times the final corona diameter during the time of its formation (i.e., a 200 km corona would require crust less than 20 km thick).

[34] Returning to the general model of corona formation in which diapirs rise through the mantle, flatten against a zone of neutral buoyancy, and impart both a structural and topographic signature on the overlying crust, we can evaluate how variations in crustal thickness might play a role in corona development and evolution. With diapir source regions located at a depth of approximately 200–250 kilometers [*Hamilton and Stofan*, 1996], individual diapir rise rates calculated on the basis of the buoyancy mechanism (either thermal or compositional) [*Hansen*, 2003], and the requirement for diapirs to achieve significant heights within the lithosphere in order to impart a surface

signature, a strong case can be made that corona-forming diapirs are compositional in nature. In such a case, the overlying crustal structure (specifically the density profile) will have a much greater effect on a diapir's ability to impart a surface signature, because neutral buoyancy zones will be established by a compositional density contrast between the mantle and the crust, rather than a temperature-dependent density contrast like the thermal lithosphere boundary or brittle-ductile transition.

## 4.2. Mechanical Strength

[35] *Koch and Manga* [1996] admit that many parameters governing the formation of corona topography are beyond our current understanding (thermal gradients and elastic properties to name a few), and by using a uniform viscosity profile, they place undesirable limits to the applicability of their models to the real world. However, mechanical yield strength envelopes for lithologies consistent with Venus's crust and mantle at a variety of thermal gradients reveal that thin crust is not only necessary to reproduce the observed topography, it also creates a favorable environment for corona structural development.

[36] Rock layer mechanical strength is affected by four principal variables: 1) composition, 2) thermal environment, 3) layer thickness, and 4) strain rate. No single variable

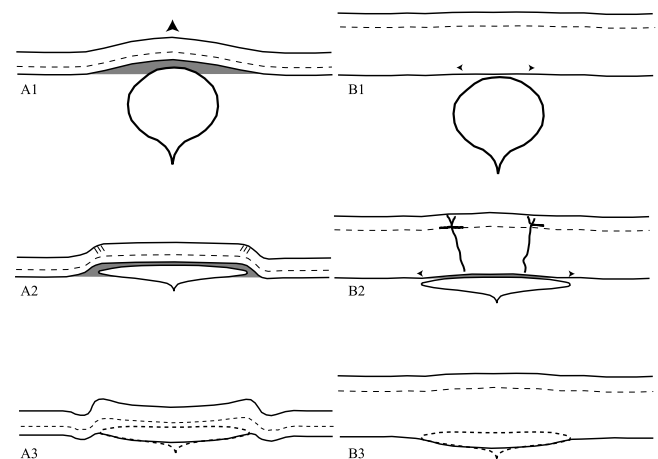


**Figure 8.** Comparison of diapir impingement at the neutral buoyancy zone of nominal (left) and thick (right) crust, dashed line represents the elastic lithosphere. Representative stages of development and are not meant to be time equivalent for each conceptual model. Diapir interaction with nominal crust is directly from corona evolution models by *Squyres et al.* [1992] and *Stofan et al.* [1997]: A1-buoyancy forced transformed into topographic uplift; this also induces partial melt generation by decompression (gray), A2-flattening and lateral spreading of diapir accompanied by continued partial melt generation and strain localization at margins, A3-interior collapse and incorporation of diapir as new crustal material. Diapir stagnation is illustrated to the right: B1-buoyancy force transmitted into lateral flow of the lower crust, B2-continued lateral flow of the lower crust, accompanied by broad regional doming, diffuse deformation, and upward migration of lowest density melts, B3-diapir is incorporated as new crustal material.

dominates across physical parameter space. However, for Venus it can be envisaged that compositional differences could play a significant role. Temperature differences are negligible, and strain rates are significantly low; therefore layer thickness (particularly crustal thickness) is important in determining the overall effective competency within the lithosphere. The term ‘competence’ can be used to describe the effect that differences in rock properties have on the development of mechanical instability [Ramsey and Huber, 1983]. Typically the term is used to evaluate rheological differences within a layered system at a small scale; however, in this case the concept refers to the lithosphere (specifically the upper and lower crust, and upper mantle). Although competence is not a direct quantitative measurement of rock strength, it can provide a comparative description of varying rock materials and their rheological response during deformation (i.e., *rock x* was more/less competent than *rock y*).

[37] Despite uncertainties of the make-up and internal crustal structure on Venus, evidence of widespread volcanic processes leads to a picture that repeated eruptions from a variety of sources have built a crust containing numerous horizontal to subhorizontal layers (underplating may also play a role in creating a horizontal layering). These volcanic layers may have slightly different compositions (i.e., tholeiitic versus alkalic, etc.), or varying degrees of vesicularity and volatile abundance, but they probably have generally similar strengths and therefore they probably do not exhibit significant strong-weak relationships as observed on Earth by the juxtaposition of drastically variable strata of similar thickness (e.g., meter-thick limestone versus meter-thick shale). Although the inter-layering of flows on Venus may be important for creating instabilities in response to lateral movements (i.e., boundary layer slip and wrinkle ridge development), they most likely do not play a role with concern to vertical tectonics associated with diapiric rise, given that layering is perpendicular to buoyancy forces of rising diapirs. In addition to the surface rocks generally having similar compositions, the scale of the processes investigated here (whole crust or whole elastic lithosphere) generally serves to average small-scale, vertical compositional heterogeneity. Therefore compositional strength differences are limited to only the crust (diabase) versus the mantle (olivine) composition and not potential intra-crustal differences.

[38] Also, temperature variations are treated as equal across all regions. With a wide range of proposed thermal gradients to choose from ( $5\text{--}30^\circ\text{C km}^{-1}$  [e.g., Solomon and Head, 1982; Johnson and Sandwell, 1994; Schubert and Sandwell, 1995]), a conservative gradient of  $10^\circ\text{C km}^{-1}$  is selected (falling within the  $8\text{--}11^\circ\text{C km}^{-1}$  of Phillips *et al.* [1997]). This value corresponds to a thermal lithosphere boundary located approximately 100 km deep and an elastic limit within the upper 20 km of the lithosphere; both values are generally accepted for the current state of Venus [Phillips *et al.*, 1997]. Evaluation of higher and lower thermal gradients affects only the depths of the various boundary layers, but does not affect the relative strength differences between the mantle and the crust. In addition, a moderate strain rate ( $10^{-15}\text{ s}^{-1}$ ) is used considering that this study is evaluating broad processes and not a particular deformational event.

[39] Choosing a  $10^\circ\text{C km}^{-1}$  geothermal gradient, a strain rate of  $10^{-15}\text{ s}^{-1}$ , and a strength depth relationship that follows Byerlee’s law, yields an elastic lithosphere thickness of approximately 11–13 kilometers for elevations near mean planetary radius. For higher elevations (given the same geothermal gradient), the elastic lithosphere is slightly thicker ( $\sim 14\text{--}16\text{ km}$ ) due to the effect of the atmospheric temperature gradient of  $\sim 8^\circ\text{C km}^{-1}$ . Below the elastic lithosphere, Mackwell *et al.*’s [1998] flow laws for dry Maryland diabase (crust) and dry olivine (mantle) [Chopra and Paterson, 1984], are used to complete three strength profiles for 10, 20, and 40 km crust (Figure 9). Although some crustal plateaus may have crustal thicknesses of 80 km or more, the strength difference between diabase and olivine is negligible below 40 km and therefore does not significantly influence surface deformation. These simple plots illustrate that in addition to increasing the depth to the neutral buoyancy zone, a thick crust on Venus results in mechanical weakening at depth. Although the overall competency of the elastic layer is practically unchanged in each case, occurring at 12–16 km depth, the response of the lower crust is significantly modified.

[40] For terrestrial continental lithospheric extension, models by Buck [1991] predict that variations in crustal thickness, or crustal component of the lithosphere (all else being equal), are the determining factor for the representative mode of extension (i.e., narrow or wide rifting, or core complex formation). This is because crust to thermal lithosphere thickness ratios control vertical viscosity profiles and the overall yield strength of deforming rock packages. With a thick crust, the lower crust is less competent (weak) and may flow rapidly, thus maintaining a relatively flat topology of the crust-mantle compositional boundary, causing widely distributed deformation. In contrast, slow flowing lower crust, or thin crust, results in strain localization and thinning of the entire crustal package. This may induce upper mantle flow, creating topologic perturbations of the thermal lithosphere, concentrating heat and strain into a narrow region. By analogy, this type of lower crust behavior may be appropriate for explaining the elastic lithosphere’s reaction to corona diapirs on Venus. Thin crust would allow a diapir to rise to sufficient levels where it may transmit stress to the elastic lithosphere, resulting in brittle surface structure development (i.e., radial and concentric fractures). Upwelling of the elastic lithosphere may also promote upper mantle flow as in the terrestrial extension case, and induce additional partial melt generation by decompression. Alternatively, thick crust distributes strain throughout the lower crust by viscous flow and minimizes partial melting. Thick crust, through time, may develop isolated perturbations that allow migration of low-density phases to the surface; however, it inhibits true corona formation by retarding the transmission of stress and melt to the upper crust as a single bulk entity.

## 5. Discussion

[41] The IKVC system and Devana Chasma, together, represent nearly one-fourth of all chasmata on Venus. Each of these chasma segments is characterized by a continuous to discontinuous topographic trough (1–4 km in depth), densely lineated terrain, and evidence of extensive volcanic

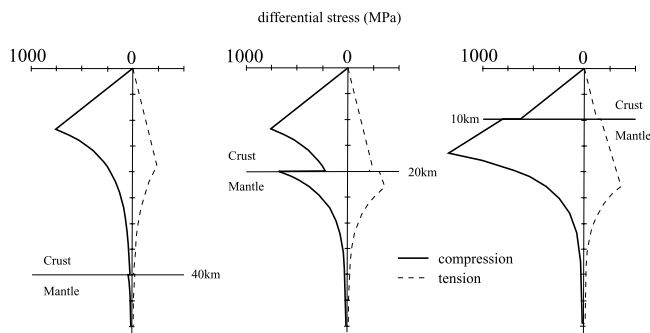


**Figure 9.** Strength envelopes derived from Byerlee's law and the creep component for a Maryland diabase crust [Mackwell *et al.*, 1998] of 40, 20, and 10 km underlain by a dry olivine mantle as a function of depth in the lithosphere with a temperature profile of  $10^{\circ}\text{C km}^{-1}$  and a strain rate of  $10^{-15}/\text{s}$ . Note that for both thick and nominal crust, the strength envelope displays a nearly uniform curve with a distinct elastic lithosphere boundary at  $\sim 13$  km and 16 km, respectively. For moderately thick crust a strong-weak-strong rheology is present, which has been used to explain multiple tectonic wavelengths of some Venusian features [Zuber, 1987; Brown and Grimm, 1995].

activity. This matches the general morphologic descriptions of Diana, Hecate, Parga, and Artemis Chasmata [Hansen and Phillips, 1993; Hamilton and Stofan, 1996; Stofan *et al.*, 2000; Hansen, 2002]. The principle difference between IKVC and Devana Chasma and the remaining chasmata is that 1) they have statistically significant negative spatial distribution correlation with the global corona population, and 2) they all are forming or have formed in regions characterized by crustal plateaus or thickened crust (e.g., Ovda, Thetis, and Phoebe regions). General observation of these areas is consistent with the present understanding of chasma formation mechanisms (limited extension accompanied by magma production and surface lava flows). However, detailed mapping reveals geologic evidence that supports the hypothesis that the morphologic differences (lack of coronae) along IKVC and Devana Chasma result from diapiric stagnation caused by interaction with thickened crust associated with ancient crustal plateaus.

[42] Crustal plateau formation imparts both mechanical and compositional crustal heterogeneities, thereby changing the lithospheric thermal structure, density stratification, and overall rheological profile. The consequence of these local and regional crustal variations 1) inhibit corona formation by diapirism by increasing the thickness and/or decreasing the density of the upper crustal layer, and 2) effectively removing the buoyancy force and therefore decreasing the transmission of stress to the elastic lithosphere by allowing increased viscous flow within the lower crust. Specific geologic features along IKVC, pseudocorona (Figures 4b–4d), lead to the proposal of the diapir stagnation model. Each of the locations reflects volcanic and tectonic elements consistent with diapir related processes, yet do not exhibit complete well-formed corona features. These pseudocorona could represent diapirs spawned by broad mantle upwelling trapped beneath or within thick crust.

[43] The presence of Verdandi Corona (Figure 4a) appears to immediately contradict the diapir stagnation model proposed herein, given that Verdandi is a well-formed corona and occurs within a crustal plateau region. However, geophysical modeling [Nunes and Phillips, 2002] and geologic mapping [Tewksbury, 2003] highlight the significance of interior crustal plateau collapse, which may indicate that through time outward viscous flow of the interior crustal plateau material destabilizes the interior and leads to sinking, while at the same time generating a compensation mechanism for upholding the marginal arcuate fold belts. A decrease in interior crustal plateau topography would suggest under-compensation and thinner interior crust, which might in turn be penetrated by later rising diapirs. In contrast, high topography preserved in central Ovda and Thetis reflects thick crust that would inhibit diapiric rise (Figure 10).

[44] Like IKVC, Devana Chasma lacks corona features. Jurdy and Stoddard [2001] hint that the lack of coronae along the Devana Chasma may indicate that Devana is less active than other chasma-coronae chains; however, this idea is inconsistent with recent analyses by Kiefer and Peterson [2003]. Kiefer and Peterson's [2003] thermal models and crustal structure analysis based on gravity-topography inversion finds that 1) thermal anomalies associated with Devana Chasma and Phoebe Regio

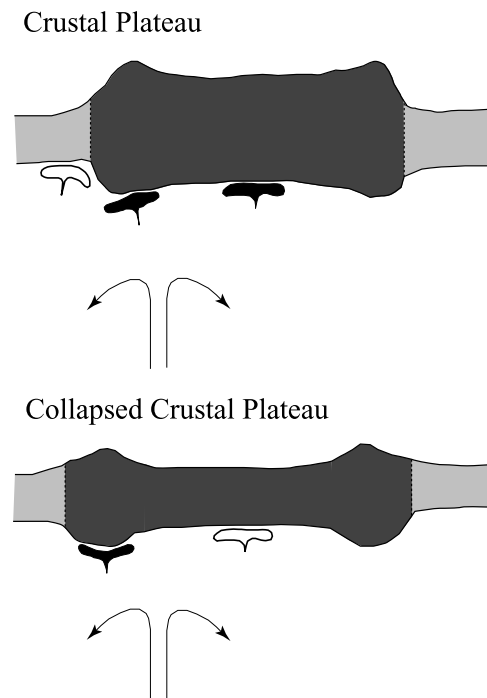


**Figure 10.** Cartoon illustrating the difference between highstanding and “collapsed” crustal plateaus. Diapir ascent is stalled (black) at deeper levels under a thick interior crustal plateau, inhibiting the development of a surface corona feature. Whereas the interior of collapsed, under-compensated, crustal plateaus may have similar crustal thickness to the surrounding plains, which do not inhibit diapir ascent (white) and corona formation. A similar thickness of collapsed crustal plateau interior and plains is supported by their similar elevation.

are indications of current upwelling consistent with proposed models of chasma formation (broad cylindrical upwelling), and 2) confirms the thickness of Phoebe Regio as ~50 km, well above the limit for corona formation by diapiric rise proposed here. Because Devana Chasma cuts through a region of thickened crust, Phoebe Regio [Grimm, 1994; Simons *et al.*, 1997], further detailed geologic mapping is necessary to investigate the applicability of the diapir stagnation model to this region. Preliminary analyses illustrate intriguing similarities to the IKVC.

## 6. Summary

[45] Detailed structural and geologic mapping techniques have been utilized to constrain simple neutral buoyancy and mechanical strength profiles. The results of which may help to explain inconsistencies in observational and statistical spatial associations of coronae and chasmata across various physiographic provinces.

[46] • Thin, or normal, crust (typical of plains regions) allows compositional diapirs to rise to sufficient levels where they may transmit stress to the elastic lithosphere, resulting in brittle surface structure development (i.e., radial and concentric fractures)

[47] • Uplift of the elastic lithosphere associated with diapiric rise may also promote upper mantle flow and induce additional partial melt generation by decompression

[48] • Thick crust (typical of crustal plateaus) distributes strain throughout the lower crust by viscous flow and minimizes partial melting

[49] • Through time, localized perturbations or predisposed conduits may allow migration of low-density phases to the surface; however, thick crust inhibits true corona formation by retarding the transmission of stress and melt to the upper crust as a single bulk entity.

[50] **Acknowledgments.** This work was supported in part by NASA grants NAG5-4562, NAG5-10586, and NAG5-12653 to Southern Methodist University and the University of Minnesota Duluth, the Department of Geosciences at Southern Methodist University, and the NASA Texas Space Grant Consortium. Discussions with Duncan Young and Rebecca Ghent, and reviews by David Williams and James Zimbelman were extremely helpful and much appreciated. This is Planetary Science Institute Contribution 370.

## References

- Anderson, E. M. (1951), *The Dynamics of Faulting and Dyke Formation With Applications to Britain*, 206 pp., Oliver and Boyd, White Plains, N. Y.
- Atkinson, B. K. (1987), Introduction to fracture mechanics and its geophysical applications, in *Fracture Mechanics of Rock*, edited by B. K. Atkinson, pp. 1–26, Academic, San Diego, Calif.
- Baer, G., G. Schubert, D. L. Bindschadler, and E. R. Stofan (1994), Spatial and temporal relations between coronae and extensional belts, northern Lada Terra, Venus, *J. Geophys. Res.*, *99*, 8355–8369.
- Baker, V. R., G. Komatsu, V. C. Gulick, and T. J. Parker (1997), Channels and Valleys, in *Venus II*, edited by S. W. Bougher, D. M. Hunten, and R. J. Phillips, pp. 757–793, Univ. of Ariz. Press, Tucson.
- Barsukov, V. L., et al. (1984), Preliminary evidence on the geology of Venus from radar measurements by the Venera 15 and 16 probes, *Geokhimiya*, *12*, 1811–1820.
- Barsukov, V. L., et al. (1986), The geology and geomorphology of the Venus surface as revealed by the radar images obtained by Venera 15 and 16, *J. Geophys. Res.*, *91*, 378–398.
- Bindschadler, D. L. (1995), Magellan: A new view of Venus geology and geophysics, *Rev. Geophys.*, *33*, 459–467.
- Bindschadler, D. L., G. Schubert, and W. M. Kaula (1992a), Coldspots and hotspots: Global tectonics and mantle dynamics of Venus, *J. Geophys. Res.*, *97*, 13,495–13,532.
- Bindschadler, D. L., A. DeCharon, K. K. Beratan, S. E. Smrekar, and J. W. Head (1992b), Magellan observations of Alpha Regio: Implications for formation of complex ridged terrains on Venus, *J. Geophys. Res.*, *97*, 13,563–13,577.
- Bleamaster, L. F., and V. L. Hansen (2001), The Kuanja/Vir-ava Chasmata: A coherent intrusive complex on Venus, *Lunar Planet. Sci. [CD-ROM]*, *XXXII*, abstract 1316.
- Bleamaster, L. F., and V. L. Hansen (2004), Geologic map of the Ovda Regio (V35) Quadrangle, Venus, *U.S. Geol. Surv. Geol. Invest. Ser.*, *I-2808*.
- Brown, C. D., and R. E. Grimm (1995), Tectonics of Artemis Chasma: A Venusian “plate” boundary, *Icarus*, *139*, 219–249.
- Buck, W. R. (1991), Modes of continental lithospheric extension, *J. Geophys. Res.*, *96*, 20,161–20,178.
- Chapman, M. G., and J. R. Zimbelman (1998), Corona associations and their implications for Venus, *Icarus*, *132*, 344–361.
- Chopra, P. N., and M. S. Paterson (1984), The role of water in the deformation of dunite, *J. Geophys. Res.*, *89*, 7861–7876.
- Copp, D. L., J. E. Guest, and E. R. Stofan (1998), New insights into corona evolution: Mapping on Venus, *J. Geophys. Res.*, *103*, 19,401–19,410.
- DeLaughter, J. E., and D. M. Jurdy (1999), Corona classification by evolutionary stage, *Icarus*, *139*, 81–92.
- Dombard, A. J., C. L. Johnson, M. A. Richards, and S. C. Solomon (2002), A transient plume melting model for coronae on Venus, *Lunar Planet. Sci. [CD-ROM]*, *XXXIII*, abstract 1877.
- Engelder, T. (1987), Joints and shear fractures in rock, in *Fracture Mechanics of Rock*, edited by B. K. Atkinson, pp. 27–69, Academic, San Diego, Calif.
- Ghent, R. R., and V. L. Hansen (1999), Structural and kinematic analysis of eastern Ovda Regio, Venus: Implications for crustal plateau formation, *Icarus*, *139*, 116–136.
- Gilmore, M. S., M. I. Ivanov, J. W. Head, and A. Basilevsky (1997), Duration of tessera deformation on Venus, *J. Geophys. Res.*, *102*, 13,357–13,368.
- Gilmore, M. S., G. S. Collins, M. A. Ivanov, L. Marinangeli, and J. W. Head (1998), Style and sequence of extensional structures in tessera terrain, Venus, *J. Geophys. Res.*, *103*, 16,813–16,840.
- Griffiths, R. W. (1986), The differing effects of compositional and thermal buoyancies on the evolution of mantle diapirs, *Phys. Earth Planet. Inter.*, *43*, 261–273.
- Grimm, R. E. (1994), The deep structure of Venusian plateau highlands, *Icarus*, *112*, 89–103.
- Grimm, R. E., and P. C. Hess (1997), The crust of Venus, in *Venus II*, edited by S. W. Bougher, D. M. Hunten, and R. J. Phillips, pp. 1205–1244, Univ. of Ariz. Press, Tucson.
- Grimm, R. E., and R. J. Phillips (1992), Anatomy of a Venusian hot spot: Geology, gravity, and mantle dynamics of Eistla Regio, *J. Geophys. Res.*, *97*, 16,035–16,054.
- Guest, J. E., and E. R. Stofan (1999), A new view of the stratigraphic history of Venus, *Icarus*, *139*, 55–66.
- Hamilton, V. E., and E. R. Stofan (1996), The geomorphology and evolution of Hecate Chasma, Venus, *Icarus*, *121*, 171–194.
- Hansen, V. L. (2002), Artemis: Surface expression of a deep mantle plume on Venus, *Geol. Soc. Am. Bull.*, *114*, 839–848.
- Hansen, V. L. (2003), Venus diapirs: Thermal or compositional?, *Geol. Soc. Am. Bull.*, *115*(9), 1040–1052.
- Hansen, V. L., and H. R. DeShon (2002), Geologic map of the Diana Chasma Quadrangle (V37), Venus, *U.S. Geol. Surv. Geol. Invest. Ser.*, *I-2752*.
- Hansen, V. L., and R. J. Phillips (1993), Tectonics and volcanism of eastern Aphrodite Terra, Venus: No subduction, no spreading, *Science*, *260*, 526–530.
- Hansen, V. L., and R. J. Phillips (1995), Formation of Ishtar Terra, Venus: Surface and gravity constraints, *Geology*, *23*, 292–296.
- Hansen, V. L., and J. J. Willis (1996), Structural analysis of a sampling of tesserae: Implications for Venus geodynamics, *Icarus*, *123*, 296–312.
- Hansen, V. L., and J. J. Willis (1998), Ribbon terrain formation, southwestern Fortuna Tessera, Venus: Implications for lithosphere evolution, *Icarus*, *132*, 332–343.
- Hansen, V. L., J. J. Willis, and W. B. Banerdt (1997), Tectonic overview and synthesis, in *Venus II*, edited by S. W. Bougher, D. M. Hunten, and R. J. Phillips, pp. 797–844, Univ. of Ariz. Press, Tucson.
- Hansen, V. L., B. K. Banks, and R. R. Ghent (1999), Tessera terrain and crustal plateaus, Venus, *Geology*, *27*, 1071–1074.
- Hansen, V. L., R. J. Phillips, J. J. Willis, and R. R. Ghent (2000), Structures in tessera terrain, Venus: Issues and answers, *J. Geophys. Res.*, *105*, 4135–4152.

- Head, J. W., and L. S. Crumpler (1987), Evidence for divergent plate-boundary characteristics and crustal spreading on Venus, *Science*, **238**, 1380–1385.
- Head, J. W., and L. Wilson (1992), Magma reservoirs and neutral buoyancy zones on Venus; Implications for the formation and evolution of volcanic landforms, *J. Geophys. Res.*, **97**, 3877–3903.
- Head, J. W., L. S. Crumpler, J. C. Aubele, J. E. Guest, and R. S. Saunders (1992), Venus volcanism classification of volcanic features and structures, associations, and global distribution from Magellan data, *J. Geophys. Res.*, **97**, 13,153–13,197.
- Herrick, R. R. (1994), Resurfacing history of Venus, *Geology*, **22**, 703–706.
- Herrick, R. R., and R. J. Phillips (1992), Geologic correlations with the interior density structure of Venus, *J. Geophys. Res.*, **97**, 16,017–16,034.
- Herrick, R. R., B. G. Bills, and S. A. Hall (1989), Variations in effective compensation depth across Aphrodite Terra, Venus, *Geophys. Res. Lett.*, **16**, 543–546.
- Janes, D. M., S. W. Squyres, D. L. Bindschadler, G. Baer, G. Schubert, V. L. Sharpton, and E. R. Stofan (1992), Geophysical models for the formation and evolution of coronae on Venus, *J. Geophys. Res.*, **97**, 16,055–16,067.
- Johnson, C., and M. A. Richards (2003), A conceptual model for the relationship between coronae and large-scale mantle dynamics on Venus, *J. Geophys. Res.*, **108**(E6), 5058, doi:10.1029/2002JE001962.
- Johnson, C., and D. T. Sandwell (1994), Lithospheric flexure on Venus, *Geophys. J. Int.*, **119**, 627–647.
- Jurdy, D. M., and M. Stefanick (1999), Correlation of Venus surface features and geoid, *Icarus*, **139**, 93–99.
- Jurdy, D. M., and P. R. Stoddard (2001), Orientation of coronae and relation to chasmata on Venus, *Lunar Planet. Sci. [CD-ROM]*, **XXXII**, abstract 1811.
- Kiefer, W. S., and K. Peterson (2003), Mantle and crustal structure in Phoebe Regio and Devana Chasma, Venus, *Geophys. Res. Lett.*, **30**(1), 1005, doi:10.1029/2002GL015762.
- Koch, D. M., and M. Manga (1996), Neutrally buoyant diapirs: A model for Venus coronae, *Geophys. Res. Lett.*, **23**(3), 225–228.
- López, I. (2002), Plume channeling as one possible mechanism for the origin of multiple coronae on Venus: A case study from the Helen Planitia Quadrangle (V52), *J. Geophys. Res.*, **107**(E11), 5116, doi:10.1029/2001JE001533.
- Mackwell, S. J., M. E. Zimmerman, and D. L. Kohlstedt (1998), High-temperature deformation of dry diabase with application to tectonics on Venus, *J. Geophys. Res.*, **103**, 975–984.
- McGill, G. E., S. J. Steenstrup, C. Barton, and P. G. Ford (1981), Continental rifting and the origin of Beta Regio, *Geophys. Res. Lett.*, **8**, 737–740.
- McKenzie, D., J. M. McKenzie, and R. S. Saunders (1992), Dike emplacement on Venus and on Earth, *J. Geophys. Res.*, **97**(E10), 15,977–15,990.
- Moore, W. B., and G. Schubert (1997), Venusian crustal and lithospheric properties from nonlinear regressions of highland geoid and topography, *Icarus*, **128**, 415–428.
- Nunes, D. C., and R. J. Phillips (2002), State of compensation and its control on the relaxation of crustal plateaus on Venus, *Lunar Planet. Sci. [CD-ROM]*, **XXXIII**, abstract 1884.
- Phillips, R. J. (1986), A mechanism for tectonic deformation on Venus, *Geophys. Res. Lett.*, **13**, 1141–1144.
- Phillips, R. J. (1990), Convection-driven tectonics on Venus, *J. Geophys. Res.*, **95**, 1301–1316.
- Phillips, R. J., and V. L. Hansen (1994), Tectonic and magmatic evolution of Venus, *Annu. Rev. Earth Planet. Sci.*, **22**, 597–654.
- Phillips, R. J., and V. L. Hansen (1998), Geologic evolution of Venus: Rises, plains, plumes, and plateaus, *Science*, **279**, 1492–1497.
- Phillips, R. J., and M. C. Malin (1984), Tectonics of Venus, *Annu. Rev. Earth Planet. Sci.*, **12**, 411–443.
- Phillips, R. J., W. M. Kaula, G. E. McGill, and M. C. Malin (1981), Tectonics and evolution of Venus, *Science*, **212**, 879–887.
- Phillips, R. J., C. L. Johnson, S. J. Mackwell, P. Morgan, D. T. Sandwell, and M. T. Zuber (1997), Lithospheric mechanics and dynamics of Venus, in *Venus II*, edited by S. W. Bougher, D. M. Hunten, and R. J. Phillips, pp. 1163–1204, Univ. of Ariz. Press, Tucson.
- Price, M., and J. Suppe (1995), Constraints on the resurfacing history of Venus from the hypsometry and distribution of volcanism, tectonism, and impact craters, *Earth Moon Planets*, **71**, 99–145.
- Ramsey, J. G., and M. I. Huber (1983), *The Techniques of Modern Structural Geology*, vol. 1, *Strain Analysis*, 307 pp., Academic, San Diego, Calif.
- Rathbun, J. A., D. M. Janes, and S. W. Squyres (1999), Formation of Beta Regio, Venus: Results from measuring strain, *J. Geophys. Res.*, **104**, 1917–1927.
- Robinson, C. A., and J. A. Wood (1993), Recent volcanic activity on Venus: Evidence from radiothermal emissivity measurements, *Icarus*, **102**, 26–39.
- Rosenblatt, P., and P. C. Pinet (1994), Comparative hypsometric analysis of Earth and Venus, *Geophys. Res. Lett.*, **21**, 465–468.
- Sandwell, D. T., and G. Schubert (1992), Evidence for retrograde lithospheric subduction on Venus, *Science*, **257**, 766–770.
- Sandwell, D. T., C. L. Johnson, F. Bilotti, and J. Suppe (1997), Driving forces for limited tectonics on Venus, *Icarus*, **129**, 232–244.
- Schaber, G. G. (1982), Venus, limited extension and volcanism along zones of lithospheric weakness, *Geophys. Res. Lett.*, **9**, 499–502.
- Schubert, G., and D. T. Sandwell (1995), A global survey of possible subduction sites on Venus, *Icarus*, **117**, 173–196.
- Simons, M., B. H. Hager, and S. C. Solomon (1994), Global variations in the geoid/topography admittance if Venus, *Science*, **264**, 798–803.
- Simons, M., S. C. Solomon, and B. H. Hager (1997), Localization of gravity and topography: Constraints on the tectonics and mantle dynamics of Venus, *Geophys. J. Int.*, **131**, 24–44.
- Smrekar, S. E., and R. J. Phillips (1991), Venusian highlands: Geoid to topography ratios and their implications, *Earth Planet. Sci. Lett.*, **107**, 582–597.
- Smrekar, S. E., and E. R. Stofan (1999), Origin of corona-dominated topographic rises on Venus, *Icarus*, **139**, 100–115.
- Smrekar, S. E., W. S. Kiefer, and E. R. Stofan (1997), Large volcanic rises on Venus, in *Venus II*, edited by S. W. Bougher, D. M. Hunten, and R. J. Phillips, pp. 845–878, Univ. of Ariz. Press, Tucson.
- Solomon, S. C. (1993), The geophysics of Venus, *Phys. Today*, **46**, 48–55.
- Solomon, S. C., and J. W. Head (1982), Mechanisms for lithospheric heat transport on Venus: Implications for tectonic style and volcanism, *J. Geophys. Res.*, **87**(B11), 9236–9246.
- Solomon, S. C., et al. (1992), Venus tectonics: An overview of Magellan observations, *J. Geophys. Res.*, **97**, 13,199–13,255.
- Squyres, S. W., D. M. Janes, G. Baer, D. L. Bindschadler, G. Schubert, V. L. Sharpton, and E. R. Stofan (1992), The morphology and evolution of coronae on Venus, *J. Geophys. Res.*, **97**, 13,611–13,634.
- Stofan, E. R., J. W. Head, D. B. Campbell, S. H. Zisk, A. F. Bogomolov, O. N. Rzhiga, A. T. Basilevsky, and N. Armand (1989), Geology of a rift zone on Venus: Beta Regio and Devana Chasma, *Geol. Soc. Am. Bull.*, **101**, 143–156.
- Stofan, E. R., V. L. Sharpton, G. Schubert, G. Baer, D. L. Bindschadler, D. M. Janes, and S. W. Squyres (1992), Global distribution and characteristics of coronae and related features on Venus: Implications for origin and relation to mantle processes, *J. Geophys. Res.*, **97**, 13,347–13,378.
- Stofan, E. R., V. E. Hamilton, D. M. Janes, and S. E. Smrekar (1997), Coronae on Venus: Morphology and origin, in *Venus II*, edited by S. W. Bougher, D. M. Hunten, and R. J. Phillips, pp. 931–965, Univ. of Ariz. Press, Tucson.
- Stofan, E. R., S. E. Smrekar, and P. Martin (2000), Coronae of Parga Chasma, Venus: Implications for chasma and coronae evolution, *Lunar Planet. Sci. [CD-ROM]*, **XXXI**, abstract 1578.
- Stofan, E. R., S. E. Smrekar, S. W. Tapper, J. E. Guest, and P. M. Grinrod (2001), Preliminary analysis of an expanded corona data base for Venus, *Geophys. Res. Lett.*, **28**, 4267–4270.
- Suppe, J., and C. Connors (1992), Critical taper wedge mechanics of fold and thrust belts on Venus: Initial results from Magellan, *J. Geophys. Res.*, **97**, 13,545–13,562.
- Tewksbury, C. M. (2003), Crustal plateau collapse on Venus: Evidence from the Pasom-Mana Region, *Lunar Planet. Sci. [CD-ROM]*, **XXXIV**, abstract 1291.
- Whitehead, J. A., and D. S. Luther (1975), Dynamics of laboratory diapir and plume models, *J. Geophys. Res.*, **80**, 705–717.
- Willis, J. J., and V. L. Hansen (1996), Conjugate shear fractures at “Ki Corona,” southeast Parga Chasma, *Lunar Planet. Sci. [CD-ROM]*, **XXVII**, 1443–1444.
- Zuber, M. T. (1987), Constraints on the lithospheric structure on Venus from mechanical models and tectonic surface features, *Proc. Lunar Planet. Sci. Conf. 17th*, Part 2, *J. Geophys. Res.*, **92**(B4), E541–E551.
- Zuber, M. T., and E. M. Parmentier (1990), On the relationship between isostatic elevation and the wavelengths of tectonic surface features on Venus, *Icarus*, **85**, 290–308.

L. F. Bleamaster III, Planetary Science Institute, 1700 East Ft. Lowell Road, Suite 106, Tucson, AZ 85719-2395, USA. (lbleamas@psi.edu)  
 V. L. Hansen, Department of Geological Sciences, University of Minnesota Duluth, Duluth, MN 55812-3036, USA. (vhansen@d.umn.edu)